Pt_3Ga: Thermodynamics and Nonstoichiometry

Agnes Schweitzer[a], Yongzhang Huang[a,c], Wenxia Yuan[b], Zhiyu Qiao[c], Olga Semenova[a], Friedrich Gehringer[a], and Herbert Ipser[a]

[a] Institut für Anorganische Chemie, Universität Wien, A-1090 Wien, Austria
[b] Department of Chemistry, University of Science and Technology Beijing, Beijing 100083, P. R. China
[c] Department of Physical Chemistry, University of Science and Technology Beijing, Beijing 100083, P. R. China

Reprint requests to Prof. Dr. H. Ipser. E-mail: herbert.ipser@univie.ac.at.

Z. Naturforsch. **59b,** 999 – 1005 (2004); received June 9, 2004

Dedicated to Professor Kurt O. Klepp on the occasion of his 60th birthday

Thermodynamic activities of gallium were measured between about 1000 and 1300 K in the non-stoichiometric intermetallic compound Pt_3Ga using an emf-method based on an oxygen conducting solid electrolyte. The variation of the lattice parameter with composition was determined by powder X-ray diffraction. The results of the activity measurements are interpreted in terms of a statistical-thermodynamic model for $L1_2$-phases considering four types of point defects, *i. e.* anti-structure atoms and vacancies on the platinum and gallium substructures. The energies of formation of the point defects at the stoichiometric composition are estimated from a curve fitting procedure yielding $E_f(Pt^{Ga}) = E_f(Ga^{Pt}) = 1.25$ eV, assuming that $E_f(V^{Pt}) = E_f(V^{Ga}) = 2.0$ eV. This results in a disorder parameter $\alpha' = 3 \cdot 10^{-6}$ at 1173 K which means that at the stoichiometric composition 0.0012% of the gallium substructure sites are occupied by platinum atoms and 0.0004% of the platinum sites by gallium atoms at this temperature.

Key words: Pt_3Ga: Thermodynamics, Pt_3Ga: Nonstoichiometry, Thermodynamic Measurements, Statistical-Thermodynamic Model, Platinum-Gallium Alloys

Introduction

In a series of investigations [1 – 5] the defect chemistry of intermetallic compounds A_3B with the ordered $L1_2$-type crystal structure has been studied. Experimental thermodynamic data, *i.e.* thermodynamic activities of the corresponding minority component, were evaluated in terms of statistical-thermodynamic model equations to obtain information on the types and concentrations of the point defects present in the crystal structure. These point defects, vacancies and anti-structure atoms (interstitial defects do not play any significant role in this type of intermetallics), exist as thermal defects at any finite temperature but also as constitutional defects that are responsible for the deviation from the exact A_3B stoichiometry.

Unfortunately, in the case of Ni_3Ga [2, 3] and Pt_3In [5] the experimental activity data were not accurate enough to warrant an evaluation of four independent parameters, *i.e.* the energies of formation of vacancies and anti-structure atoms on the two substructures (the Ni (Pt) and Ga (In) substructure), by means of the statistical-thermodynamic model. Therefore it was assumed that, similar as in the Ni_3Al compound [1], the energies of formation of the vacancies are considerably higher than those of the anti-structure atoms, and they were set equal at 2.0 eV. Assuming furthermore that the energies of formation of the anti-structure defects are also roughly equal, it was possible to derive the corresponding values by a curve fitting procedure, arriving at values of 0.60 eV for Ni_3Ga and 1.15 eV for Pt_3In. The results were basically confirmed in their trends by accompanying *ab initio* calculations of the different defect formation energies [6, 7] although the absolute values were somewhat different.

In the Pt-Ga phase diagram [8], a compound γ-Pt_3Ga (from here on simply Pt_3Ga) with a crystal structure of the $L1_2$-type is reported to exist at temperatures up to 1374 °C with a maximum homogeneity range between 24 and 32 at-% Ga. Since no information on the defect chemistry of this compound could be found in the literature it was decided to apply the

statistical-thermodynamic model equations [1] to experimental thermodynamic data and to estimate in this way values for the energies of formation of the different point defects (anti-structure platinum and gallium atoms, platinum and gallium vacancies). With these it would be possible to calculate the defect concentrations as functions of temperature and composition and to determine those defects that are mainly responsible for nonstoichiometry.

Due to the scarcity of thermodynamic information for Pt_3Ga in the literature (three data points for the gallium activity by Katayama *et al.* [9]) the necessary thermodynamic data had to be determined experimentally by means of an electromotive force (emf) method using a solid oxygen conducting electrolyte. Two separate experimental setups, although of nearly identical design, were used in Beijing and Vienna to obtain the thermodynamic activity of gallium as a function of temperature between 20 and 32 at-% Ga. In the following, the two separate data sets are combined and evaluated together to obtain the partial Gibbs energy, *i. e.* the thermodynamic activity of gallium in the given composition range. The composition dependence of the gallium activity at a given temperature is evaluated in terms of the statistical-thermodynamic model equations in order to estimate the energies of formation of the individual point defects.

Experimental Procedure

Experimental principles

The solid state galvanic cells used for the determination of the thermodynamic properties of the Pt_3Ga-phase as a function of temperature and composition were based on the principles outlined by Kiukkola and Wagner [10]. Measuring the emf of a cell

$$\text{(-)Ga, } Ga_2O_3 \,|\, ZrO_2(Y_2O_3) \,|\, Pt_3Ga, Ga_2O_3(+) \qquad (1)$$

as a function of temperature, one can derive all partial thermodynamic quantities, *i. e.* $\Delta\bar{G}_{Ga} = RT\ln a_{Ga}$, $\Delta\bar{H}_{Ga}$, and $\Delta\bar{S}_{Ga}$. Since elemental Ga, at the temperatures of interest (1000 – 1300 K), is in the liquid state one often resorts to a cell of the type

$$\text{(-) } Pt_3Ga, Ga_2O_3 \,|\, ZrO_2(\text{ stab.}) \,|\, Fe, Fe_xO(+) \qquad (2)$$

The measured emf-values can be combined with those of the cell

$$\text{(-) Ga, } Ga_2O_3 \,|\, ZrO_2(\text{ stab.}) \,|\, Fe, Fe_xO(+) \qquad (3)$$

which were reported by Katayama *et al.* [11] as

$$E_{(3)}/\text{V} = 0.51962 - 2.322\cdot 10^{-4}\,T/\text{K} \qquad (4)$$

(with an uncertainty of ± 1.39 mV) to give the emf of the hypothetical cell (1). For the corresponding cell reaction the change in the partial Gibbs energy of formation is given by

$$\Delta\bar{G}_{Ga} = \bar{G}_{Ga} - G^{o}_{Ga} = -3EF = RT\ln a_{Ga} \qquad (5)$$

where E is the emf of cell (1) in V, F is the Faraday constant, R is the gas constant, a_{Ga} is the thermodynamic activity of Ga in Pt_3Ga, and T the temperature in K. From the temperature dependence of the emf the other partial properties can be derived:

$$\Delta\bar{S}_{Ga} = 3F\left(\frac{\partial E}{\partial T}\right) \qquad (6)$$

$$\Delta\bar{H}_{Ga} = 3F\left[T\left(\frac{\partial E}{\partial T}\right) - E\right] \qquad (7)$$

Experimental procedure

The experimental setup used for the emf measurements, both in Vienna (Series A) and in Beijing (Series B), was described in detail by Yuan *et al.* [3]. For series A, altogether fourteen samples were prepared in the composition range between 20 and 32 at-% Ga; their nominal compositions are given in Table 1. Starting materials for all samples were Pt (wire, 1 mm diameter, 99.95%; ÖGUSSA, Vienna, Austria) and Ga (splatters, 99.9999%; Alpha, Karlsruhe, Germany). Appropriate amounts of the pure elements were weighed and mixed and thereafter melted under Ar atmosphere in an arc furnace on a water cooled copper hearth. They were re-melted several times to guarantee homogeneity. The total mass of each sample was about 3 g. In order to check for any mass losses all samples were reweighed, and samples with losses of more than 0.5% were discarded resulting in composition values with uncertainties of better than ± 0.5 at%. (The same was done for samples of series B.) The resulting ingots were pulverized in a tungsten carbide mortar, the powders were sealed under vacuum (approx. 10^{-3} mbar) in quartz ampoules, annealed at 1073 K for 35 days and quenched.

All samples were subjected to X-ray powder diffraction to confirm the corresponding phase composition. For this purpose a Guinier-Huber camera was employed using Cu-K_α radiation with high purity Si as internal standard. The lattice parameters of the cubic $L1_2$-Pt_3Ga-phase were calculated from the spacings of the diffraction lines by means of the software package “Struktur” [14].

The sample electrodes for the emf-measurements were prepared by mixing the alloy powders with Ga_2O_3 (powder, 99.99%; Aldrich, Vienna) in a mass ratio m(alloy): $m(Ga_2O_3)$ = 7:1. These mixtures were pressed into pellets under a pressure of about 5 GPa. The reference electrode (Fe, Fe_xO) was prepared by mixing two parts of Fe powder (99.5%) with one part of Fe_2O_3 powder (99.5%; both Alfa

Table 1. Experimental results of the emf-measurements of cell (2) and calculated emf of the hypothetical cell (1).

Sample composition, x_{Ga}	Phase composition	T(K)	$(E/\mathrm{V}) = A + B\cdot(T/\mathrm{K})$ cell (2) A	cell (2) $B\cdot10^3$	cell (1) A	cell (1) $B\cdot10^3$
Series A: measurements in Vienna						
0.20	Pt+Pt_3Ga	1083 – 1230	0.0664	−0.2826	0.4532	0.0504
0.21	Pt+Pt_3Ga	1089 – 1239	0.0474	−0.2653	0.4722	0.0331
0.22	Pt+Pt_3Ga	1096 – 1244	0.0959	−0.3103	0.4237	0.0781
0.25	Pt_3Ga	1011 – 1169	0.2104	−0.3429	0.3092	0.1107
0.255	Pt_3Ga	1090 – 1236	0.0694	−0.1922	0.4502	−0.0400
0.265	Pt_3Ga	1100 – 1241	0.0402	−0.1773	0.4794	−0.0549
0.275	Pt_3Ga	1076 – 1234	0.0861	−0.2008	0.4335	−0.0314
0.28	Pt_3Ga	1023 – 1220	0.0765	−0.1627	0.4431	−0.0695
0.285	Pt_3Ga	1092 – 1260	0.0364	−0.1187	0.4832	−0.1135
0.29	Pt_3Ga	1095 – 1265	0.0369	−0.1098	0.4872	−0.1224
0.295	Pt_3Ga	1066 – 1238	0.0233	−0.1168	0.4963	−0.1154
0.30	Pt_3Ga	1008 – 1258	0.0422	−0.1293	0.4774	−0.1029
0.31	Pt_3Ga+ Pt_2Ga	1093 – 1240	0.0472	−0.1397	0.4724	−0.0925
0.32	Pt_3Ga+ Pt_2Ga	1097 – 1245	0.0636	−0.1307	0.4560	−0.1015
Series B: measurements in Beijing						
0.23	Pt+Pt_3Ga	1088 – 1274	0.0647	−0.2812	0.4549	0.0499
0.24	Pt+Pt_3Ga	1087 – 1273	0.0627	−0.2770	0.4570	0.0448
0.245	Pt_3Ga	1067 – 1285	0.0862	−0.2703	0.4334	0.0381
0.25	Pt_3Ga	1065 – 1282	0.1094	−0.2856	0.4102	0.0534
0.255	Pt_3Ga	1054 – 1283	0.1244	−0.2698	0.3953	0.0376
0.26	Pt_3Ga	1070 – 1281	0.1287	−0.2651	0.3910	−0.0329
0.27	Pt_3Ga	1069 – 1283	0.1078	−0.2314	0.4119	−0.0008
0.28	Pt_3Ga	1077 – 1279	0.1133	−0.2128	0.4064	−0.0194

Aesar, Vienna); it was pressed and sintered in the same way. Small crucibles made from yttria stabilized zirconia (Nikkato Corp., Japan; 12 mm o.d., 9 mm i.d., 12 mm height) served as oxygen conducting electrolyte.

A second series of experiments (Series B) was carried out in Beijing. The eight samples of Pt-Ga alloys with compositions between 23 and 28 at-% Ga and the corresponding electrodes were prepared in an analogous way. The metals and metal oxides for the electrodes were from Beijing Chemical Agent Company (Beijing, P.R. China): Pt (99.99%), Fe powder (99.99%), Ga_2O_3 powder (99.999%), and Fe_2O_3 powder (99.999%). The same type of crucibles as for series A was used as electrolyte.

In order to check for any problems that might be caused by using platinum as lead wire in the experiments (for example, by a sudden drop of the platinum activity at the interface between the Pt wire and the (Pt_3Ga, Ga_2O_3) electrode) a small piece of iridium foil (0.1 mm, 99.995%; ÖGUSSA, Vienna, Austria) was inserted between the contact wire and the measuring electrode itself in series B. Earlier experiments with the intermetallic compound Pt_3In had shown that iridium was the material best suited for that purpose [5]. Any details of the setup are also given in Ref. [5]. As it turned out, the results obtained with the samples of series B were, within the error limits, in good agreement with the results of series A.

In all experiments the reproducibility of the obtained emf values at a given temperature was checked at least once for each sample by either short circuiting the cell or by application of an external potential to the cell for a few moments. In all cases the emf returned to the original value after less than one hour, indicating that the cell assembly had in fact been in thermodynamic equilibrium. In addition, selected Pt_3Ga-Ga_2O_3 working electrodes were subjected to X-ray analysis after the emf-measurements; no change of the phase composition could be detected.

Experimental Results

Partial thermodynamic properties

The performance of the galvanic cells and the entire experimental setups was tested by measuring the emf of the cell

$$\text{(-) Fe, } Fe_xO \,|\, ZrO_2(Y_2O_3) \,|\, \text{Ni, NiO}(+) \qquad (8)$$

in the corresponding temperature ranges of the experiments, and the agreement of the obtained emf values with literature values [10, 12, 13] was good.

The results of the emf-measurements of cell (2) are listed in Table 1 together with the individual sample compositions and the phases that had been identified; the emf values are given as a function of temperature in the form $(E/\mathrm{V}) = A + B\cdot(T/\mathrm{K})$. In addition, the table contains also the emf values of the hypothetical cell (1) obtained by combining the results of cell (2) with eq. (4). From these all partial thermodynamic properties of gallium can be calculated. Fig. 1

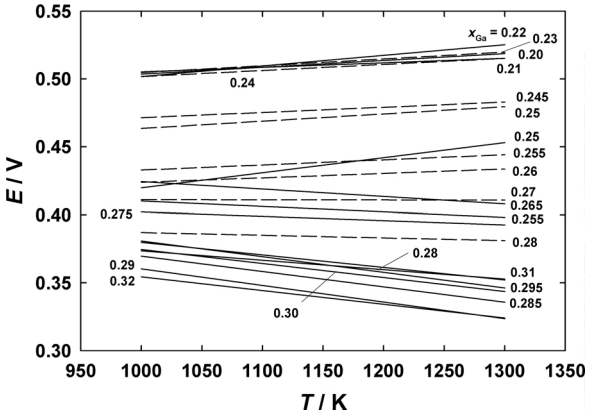

Fig. 1. Temperature dependence of the emf values of the hypothetical cell (1).

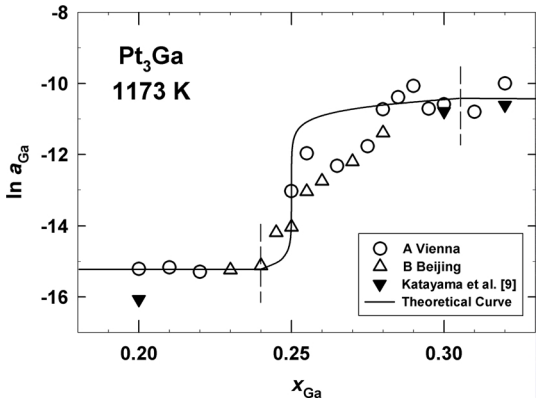

Fig. 2. Thermodynamic activity of gallium at 1173 K in the Pt_3Ga phase and neighboring two-phase fields and comparison with literature values by Katayama *et al.* [9]; the full line was obtained from the statistical-thermodynamic model (*cf.* text).

shows the temperature dependence of the emf of the hypothetical cell (1) for both series of samples.

Fig. 1 gives also an indication of the consistency of the various experiments. Even if some scatter can be observed among the individual results for different compositions there is a clear general trend, with the slope shifting from positive for $x_{Ga} < 0.26$ to negative for $x_{Ga} > 0.26$, and with the absolute values of the emf clearly decreasing as the gallium content increases.

Partial Gibbs energies of formation and gallium activities were calculated for 1173 K. Fig. 2 shows the natural logarithm of the activity values as a function of composition together with data points by Katayama *et al.* [9]. The platinum-rich phase boundary at the given temperature was taken from the compilation by Massalski *et al.* [8]; however, the gallium-rich limit was shifted to about 30.5 at-% Ga since there are strong indications (see below) that the phase is somewhat more narrow at 1173 K than shown in Ref. [8].

Lattice parameters and homogeneity range

The results of the lattice parameter measurements for samples annealed at 1073 K are shown in Fig. 3. Originally, samples with compositions between 20 and 32 at-% Ga had been subjected to X-ray powder diffraction. However, at lower temperatures (below 255 °C) the $L1_2$-compound γ-Pt_3Ga shows a martensitic transformation in the platinum-rich region, first into β-Pt_3Ga (with a $D0_c$-type structure), and then into α-Pt_3Ga (with a $D0_c$' structure) [8, 15]. As it had been observed earlier, it is virtually impossible to quench γ-Pt_3Ga in the composition range where it shows this martensitic transformation, at least with usual quenching rates, and all samples up to 26 at-% Ga showed the X-ray powder patterns of α-Pt_3Ga. Therefore, no lattice parameters of the $L1_2$-phase could be determined for compositions below 26.5 at-% Ga.

The powder patterns of alloys with compositions up to 24 at-% Ga contained also lines of the *fcc* solid solution of (Pt) whereas for samples with 31 and 32 at-% Ga the lines of Pt_2Ga could be identified together with the strongest lines of γ-Pt_3Ga. In combination with the results of the emf-measurements, this suggests a homogeneity range for Pt_3Ga from 24 to 30.5 at-% Ga at 1073 K, somewhat more narrow on the gallium-rich side than given in Massalki's compilation [8].

It can be seen that the lattice parameter decreases smoothly within the homogeneity range of Pt_3Ga. Considering that anti-structure atoms are responsible for non-stoichiometry (see below), this is in accord with the relative sizes of the gallium and platinum atoms [16].

Discussion

Comparison with literature data

Three data points for the gallium activity at 20, 30, and 32 at-% Ga, resp., by Katayama *et al.* [9] are included in Fig. 2; it can be seen that the agreement is excellent on the gallium-rich side, whereas Katayama's value on the platinum-rich side is somewhat more negative. No other partial thermodynamic values are available in the literature.

A lattice parameter value of $a = 3.892$ Å was given by Bhan and Schubert [17] for an alloy $Pt_{75}Ga_{25}$, quenched from 993 K, which is considerably lower than the extrapolated value found here. On the other hand, we were not able to quench the $L1_2$-phase at this composition (see above) which might indicate that the gallium content in Ref. [17] was actually somewhat

Table 2. Defect formation energies for different $L1_2$-compounds*.

Comp.	$E_f(V^A)$	$E_f(V^B)$	$E_f(A^B)$	$E_f(B^A)$	α'	Ref.
Ni_3Al	1.48	2.14	0.31	0.66	$7.5\cdot10^{-3}$	1, 22
Ni_3Ga	1.5	2.0	0.6	0.6	$9\cdot10^{-4}$	3
Pt_3Ga	2.0	2.0	1.25	1.25	$3\cdot10^{-6}$	present
Pt_3In	2.0	2.0	1.15	1.15	$5\cdot10^{-6}$	5

* A = Ni, Pt; B = Al, Ga, In.

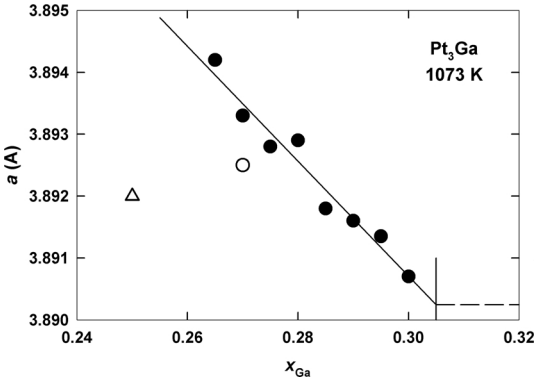

Fig. 3. Lattice parameter of Pt_3Ga for samples annealed at 1073 K as a function of composition: •, own values; △, Bhan and Schubert [17]; ○, Oya *et al.* [15].

higher. The value given by Oya *et al.* for 27 at-% Ga in their Table 2 [15], calculated for a hypothetical tetragonal cell, can be converted to $a = 3.8925$ Å for the cubic unit cell which is in good agreement with the lattice parameter found in the present investigation.

Statistical-thermodynamic evaluation

A statistical-thermodynamic model for nonstoichiometric $L1_2$-type phases was derived by Krachler *et al.* [1] based on the principles outlined earlier for B2-phases by Krachler and Ipser [18]. The crystal structure of an A_3B crystal is divided into two substructures, the A-substructure consisting of the face-centered positions in the cubic unit cell and the B-substructure consisting of the corner positions. Four types of point defects are allowed in the crystal, *i. e.* anti-structure atoms and vacancies on both substructures. Starting from the grand partition function and using a Wagner-Schottky approach [19] (*i. e.* assuming isolated point defects where the introduction or removal of any additional defect of a given type causes the same change in the internal energy independently of the numbers of point defects that are already present), equations were derived for the composition dependence of the defect concentrations and the thermodynamic activities of the components. As variable parameters the energies of formation of the point defects at the stoichiometric composition were used as defined, for example, by Gao *et al.* [20]:

$$E_f(A^B), E_f(B^A), E_f(V^A), E_f(V^B),$$

which are, in the corresponding sequence, the energies of formation of an anti-structure A-atom, an anti-structure B-atom, a vacancy on the A-substructure, a vacancy on the B-substructure. The model was applied to experimental activity values for Ni_3Al that were available in the literature using various sets of defect formation energies, also from the literature, that had been obtained by different theoretical approaches. By comparing statistical-theoretical activity curves with experimental values the optimum set of defect formation energies was derived [1].

In order to estimate the point defect formation energies for Pt_3Ga which are not available in the literature, the same model equations were applied to the gallium activity data obtained in the present investigation. Considering the situation in the structurally related compounds Ni_3Al [1], Ni_3Ga [2, 3], and Pt_3In [5], it was assumed that the energies to form vacancies would be considerably larger than those to create anti-structure defects. Therefore a value of 2.0 eV was taken as a reasonable estimate for the vacancy formation energies on both substructures. With a simple curve fitting procedure the following set of energy parameters was obtained:

$$E_f(Pt^{Ga}) = E_f(Ga^{Pt}) = 1.25 \text{ eV},$$
$$E_f(V^{Pt}) = E_f(V^{Ga}) = 2.0 \text{ eV}.$$

(It should be pointed out that for the situation of rather high energies of formation and correspondingly very small concentrations of vacancies, as in the present case, the shape of the theoretical curve becomes very sensitive to variations in the formation energies of the anti-structure defects whereas the vacancy formation energies should be considered reasonable estimates).

It is interesting to observe that the data points between 25 and 28 at-% Ga show a noticeable deviation from the theoretical curve to more negative values. A somewhat similar effect had been observed earlier for the case of Ni_3Ga [3]. Any attempt to find parameter values that would describe the data points in a better way yielded completely unreasonable combinations, like energies of formation of platinum and gallium

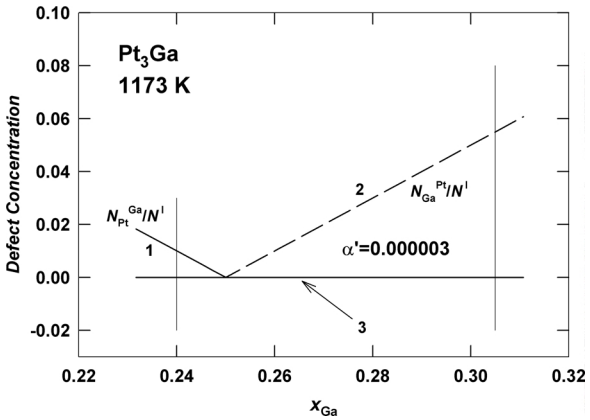

Fig. 4. Point defect concentrations (referred to the total number of lattice sites) in Pt_3Ga at 1173 K as a function of composition; 1: concentration of anti-structure platinum atoms; 2: concentration of anti-structure gallium atoms; 3: concentration of platinum and gallium vacancies (coinciding with the axis since they are several orders of magnitude smaller).

anti-structure atoms that were different by one order of magnitude. This was considered unrealistic. Even with the assumption of an uncertainty of ± 0.5 at-% in the composition and of ± 0.5 in the value of $\ln a_{\mathrm{Ga}}$ the data points would still be off the theoretical curve. On the other hand, from the values in the neighboring two-phase fields, ((Pt)+Pt_3Ga) and (Pt_3Ga+Pt_2Ga), which are well supported by the literature values [9] the height of the step function can be fixed in a very reliable way leading to rather accurate values of $E_{\mathrm{f}}(\mathrm{Pt^{Ga}})$ and $E_{\mathrm{f}}(\mathrm{Ga^{Pt}})$ if they are assumed to be equal. Thus the reason of this deviation is not clear at the moment.

Based on the derived energies of formation of the four types of point defects, the variation of their concentrations with composition could be calculated, and the result for 1173 K is shown in Fig. 4. It can be seen that the deviation from stoichiometry is in principle caused entirely by anti-structure atoms whereas vacancies play a negligible role (as was to be expected from the rather high values of the energies of formation of vacancies that had been selected). The vacancy concentrations are of the order of 10^{-6} to 10^{-12} and the corresponding curves coincide with the horizontal axis in Fig. 4 due to the selected scale. From the curves for the anti-structure Pt- and Ga-atoms a disorder parameter $\alpha' = 3 \cdot 10^{-6}$ can be derived for 1173 K where α' is defined as the concentration of anti-structure defects at the exactly stoichiometric composition [21],

$$\alpha' = (N_{\mathrm{Pt}}{}^{\mathrm{Ga}}/N^{\mathrm{l}})_{\mathrm{stoich}} = (N_{\mathrm{Ga}}{}^{\mathrm{Pt}}/N^{\mathrm{l}})_{\mathrm{stoich}}$$

with $N_{\mathrm{Pt}}{}^{\mathrm{Ga}}$ and $N_{\mathrm{Ga}}{}^{\mathrm{Pt}}$ being the numbers of anti-structure gallium or platinum atoms, respectively, and N^{l} being the total number of positions. Regarding the individual substructures, one finds that at the exactly stoichiometric composition 0.0012% of the gallium sites are occupied by platinum atoms and 0.0004% of the platinum sites by gallium atoms at this temperature.

Comparison with other $L1_2$-compounds

In recent years we investigated several intermetallic compounds with the ordered $L1_2$-type structure, and the thermodynamic activities of the minority components were evaluated in terms of the statistical-thermodynamic model of Krachler *et al.* [1]. The different compounds are listed in Table 2 together with the resulting defect formation energies. For Ni_3Al six different sets of values of these defect formation energies were available in the literature, and they were used to calculate six different theoretical activity curves. From a comparison with experimental aluminum activities by Steiner and Komarek [23] and Hilpert *et al.* [24] it was found that the values by Debiaggi *et al.* [22] which are listed in the table gave the best agreement.

In the case of Ni_3Ga and Pt_3In, a similar procedure was applied as in the present study. In analogy to Ni_3Al it was assumed that the vacancy concentrations were much smaller than those of the anti-structure defects. With reasonable assumptions about the values of the vacancy formation energies it was possible to estimate the energies of formation of the anti-structure atoms from a simple curve fitting procedure, assuming that they would be roughly equal for the two types of anti-structure defects in a particular compound.

It can be seen that the energies of formation for anti-structure atoms are considerably higher for the two compounds containing platinum than for Ni_3Al and Ni_3Ga, resulting also in a much smaller disorder parameter α'. This reflects a much higher degree of order in the two platinum compounds which must be due to a noticeably tighter chemical bonding in these latter compounds.

Acknowledgements

Financial support of the Austrian Science Foundation (FWF: Project Nos. P12962-CHE, P14519-CHE, and 16498-N10) and of the National Natural Science Foundation of China (NSFC: Project No. 29871005) as well as support by the OAD (Austrian Academic Exchange Service, Technical-Scientific Cooperation Austria-China: Project No. VI.B.7) is gratefully acknowledged.

[1] R. Krachler, O. P. Semenova, H. Ipser, Phys. Stat. Sol. (b) **216**, 943 (1999).
[2] O. P. Semenova, W. Yuan, R. Krachler, H. Ipser, Scripta Mater. **42**, 567 (2000).
[3] W. Yuan, O. Diwald, A. Mikula, H. Ipser, Z. Metallkd. **91**, 448 (2000).
[4] H. Ipser, O. P. Semenova, R. Krachler, A. Schweitzer, W. Yuan, M. Peng, Z. Qiao. In: High Temperature Ordered Intermetallic Alloys IX. MRS Symp. Proc. Vol. 646, pp. N6.11.1-6, Mater. Res. Soc., Warrendale, PA (2001).
[5] A. Schweitzer, X. Wu, W. Yuan, Y. Huang, J. Dischinger, H.-J. Schaller, Z. Qiao, F. Gehringer, H. Ipser, Intermetallics **12**, 401 (2004).
[6] H. Schweiger, O. Semenova, W. Wolf, W. Püschl, W. Pfeiler, R. Podloucky, H. Ipser, Scripta Mater. **46**, 37 (2002).
[7] W. Wolf, H. Schweiger, J. Houserova, R. Podloucky, Research in progress, University of Vienna (2004).
[8] T. B. Massalski, H. Okamoto, P. R. Subramanian, L. Kacprzak (Eds.), Binary Alloy Phase Diagrams, 2nd Ed., p. 1840, ASM International, Materials Park, OH (1990).
[9] I. Katayama, T. Makino, T. Iida, High Temp. Mater. Sci. **34**, 127 (1995).
[10] K. Kiukkola, C. Wagner, J. Electrochem. Soc. **104**, 308 (1957).
[11] I. Katayama, Sh. Igi, Z. Kozuka, Trans. Japan. Inst. Met. **15**, 447 (1974).
[12] G. G. Charette, S. N. Flengas, J. Electrochem. Soc. **115**, 796 (1968).
[13] R. Prasad, F. Sommer, J. Alloys Comp. **200**, 69 (1993).
[14] W. Wacha, Programmpaket "Struktur", Technical University of Vienna (1989), Diplomarbeit (Master Thesis).
[15] Y. Oya, Y. Mishima, T. Suzuki, Z. Metallkd. **78**, 485 (1987).
[16] J. Emsley, The Elements, Clarendon Press, Oxford (1989).
[17] S. Bhan, K. Schubert, Z. Metallkd. **51**, 327 (1960).
[18] R. Krachler, H. Ipser, Intermetallics **7**, 141 (1999).
[19] C. Wagner, W. Schottky, Z. Physik. Chem. B **11**, 163 (1931).
[20] F. Gao, D. J. Bacon, G. J. Ackland, Phil. Mag. A **67**, 275 (1993).
[21] Y. A. Chang, J. P. Neumann, Prog. Solid St. Chem. **14**, 221 (1982).
[22] S. B. Debiaggi, P. M. Decorte, A. M. Monti, Phys. Stat. Sol. (b) **195**, 37 (1996).
[23] A. Steiner, K. L. Komarek, Trans. Met. Soc. AIME **230**, 786 (1964).
[24] K. Hilpert, M. Miller, H. Gerads, H. Nickel, Ber. Bunsenges. Phys. Chem. **94**, 40 (1990).